Volume 8, Issue 3, 2019, 604 - 612 ISSN 2284-6808
Letters in Applied NanoBioScience
www.NanoBioLetters.com
https://doi.org/10.33263/LIANBS83.604612
Original Research Article Open Access Journal
Received: 04.08.2019 / Revised: 25.08.2019 / Accepted: 27.08.2019 / Published on-line: 29.08.2019

Revisiting the Hodgkin-Huxley and Fitzhugh-Nagumo models of action potential propagation

Abraham Tsitlakidis [1, 2], Nicolas Foroglou [2], Elias C. Aifantis [1]
[1]School of Engineering, Aristotle University of Thessaloniki, Thessaloniki 54124, Greece
[2]Medical School, Aristotle University of Thessaloniki, Thessaloniki 54636, Greece
*corresponding author e-mail address: ***mom@mom.gen.auth.gr*** | Scopus ID: 34871245600

ABSTRACT
The influence of neuron mechanical deformation on the generation and propagation of the action potential is studied by revisiting the Hodgkin-Huxley (H-H) and the Fitzhugh-Nagumo (F-N) models within a coupled electromechanical framework. More specifically, effects of flexoelectricity and cellular membrane deformation on the kinetics of potassium channels are studied. Their activation and inactivation rate, as well as the appearance of time delay, are considered to describe changes in the propagation velocity of the action potential due to the axon deformation. The results obtained are supported by experimental evidence, although such phenomena are extremely challenging to analyze with existing tools. The electromechanical consideration of the generation and propagation of the action potential is a very promising field with important clinical implications and wide perspectives for further understanding the pathophysiology of various neurological disorders.
Keywords: *action potential, dynamical systems, delay differential equations, electro-mechanical models.*

1. INTRODUCTION
The components of the nervous system undergo destructive or non-destructive mechanical deformation in the course of various diseases or manipulations during neurosurgical operations. For instance, the fibers of peripheral nerves may undergo compression. The result of this deformation, in addition to ischaemia, hypoxia, and non-reversible lesion, might manifest as neuroapraxia, which can be reversed by eliminating the cause of the compression. Furthermore, an increase of the intracranial pressure, as in cerebral oedema or hydrocephalus, causes changes in brain tissue perfusion, resulting in hypoxia and secondary apoptosis of the neurons that influence cerebral function. Despite all this, a least studied factor in the pathophysiology of increased intracranial pressure is the mechanical deformation of neurons and the influence that it may have on their function, i.e. the generation and propagation of the action potential. Finally, it should also be pointed out that the study of the local deformation of neural tissue, caused by tumors, surgical manipulations, or the presence of artificial implants, is of relevance here, as it may have consequences for the function of neurons.

In view of the above introductory remarks, we proceed first with the basics of earlier proposed action potential propagation models: the Hodgkin-Huxley (H-H) model and its successor commonly known as the Fitzhugh-Nagumo (F-N) model. In particular, the H-H model is reviewed in Section 2.1 and the F-N model is discussed in more detail in Section 2.2. In Section 2.3, a brief discussion of Lord Kelvin's cable theory for the nerve stimulation propagation is given. Next, in Section 2.4, electromechanical models for nerve stimulation propagation are presented by also considering the effects of flexoelectricity and time delay. Finally, in Section 3, a discussion on experiments, clinical implications, and future directions is provided.

2. EXPERIMENTAL SECTION
2.1. The Hodgkin-Huxley Model.
The action potential (the electric signal transferred by the neurons) is essentially a reversal of the polarity of the resting potential of the neurons. The generation of the action potential is usually described by a dynamical system. A dynamical system is composed of a set of state variables, corresponding to the vector $\mathbf{p}(t)$, and a rule that describes the evolution of these variables in time. The state may depend on certain parameters, which correspond to the vector **a** [1, 2]. The most distinguished such model is the one proposed in the 1950s by Hodgkin and Huxley (the H-H Nobel prize winner model), based on experiments conducted on giant squid axons [3-7]. It has established the theoretical foundations for modern neuroscience, based on the existence and function of voltage-sensitive channels specialized for each type of ion.

In this model, all factors taking part in electrical perturbations are elements of an electric circuit. The cellular membrane is regarded as a capacitor of capacitance C_m through which current I_{Cm} passes, as two conductors (intracellular and extracellular aqueous environment) are separated by a dielectric (lipid bilayer). The channels are regarded as resistors of conductivity G_K (voltage-sensitive K^+ channels), G_{Na} (voltage-sensitive Na^+ channels) and G_L (leakage channels), that are constantly open - mainly Cl^- channels of very small conductance. Through them, ion currents I_K, I_{Na} and I_L pass respectively (the ions that pass through the membrane). The sources $E_K = -77mV$,

E_{Na} = 50mV and E_L = -54.4mV that represent the respective equilibrium potentials are connected in series with the channels. The total current that passes through the membrane is $I_m = 0\mu A$ / cm^2 *in vivo*. It may be non-zero *in vitro*, when a stimulus is used experimentally to provoke the generation of the action potential. The resting potential is V_{rest} = -65mV.

The currents (in μA/cm^2) are described by the equations

$$I_{Cm} = C_m \frac{dV_m}{dt} \quad (1),$$

$$I_K = G_K\left(V_m - E_K\right) = g_K P_K\left(V_m - E_K\right) \quad (2),$$

$$I_{Na} = G_{Na}\left(V_m - E_{Na}\right) = g_{Na} P_{Na}\left(V_m - E_{Na}\right) \quad (3),$$

$$I_L = G_L\left(V_m - E_L\right) \quad (4),$$

$$I_m = I_{Cm} + I_K + I_{Na} + I_L . \quad (5)$$

The parameters $C_m = 1\mu F$ / cm^2 is the membrane capacitance (as a capacitor); $G_L = R^{-1} = 0.3mS$ / cm^2 is the leakage channel conductivity; g_K = 36mS / cm^2 and g_{Na} = 120mS / cm^2 are the K^+ and Na^+ channel special conductivities; and P_K and P_{Na} denote the open channel proportion of each type.

During action potential evolution, the opening of the voltage-gated Na^+ channels allows the influx of Na^+ ions into the cytoplasm, resulting in the reversal of the resting potential (depolarization). In consequence, opening of the voltage-gated K^+ channels, while Na^+ channels close, gradually restores the membrane potential to its resting value (repolarization). Each voltage-gated K^+ channel consists of 4 identical n gates and each Na^+ channel consists of 3 m (activation) gates and 1 h (inactivation) gate. Each gate follows a two-state (open or closed) model. All gates should be simultaneously open, in order to keep a channel open. Therefore, the proportion parameters $0 \le P_K, P_{Na} \le 1$ of open K^+ and Na^+ channels are given by the expressions

$$P_K = nnnn = n^4 \quad (6),$$

$$P_{Na} = mmmh = m^3 h \quad (7),$$

where $0 \le n, m, h \le 1$ denote the probabilities of each type of gate to be open. Combining equations (1) - (7) we obtain

$$I_m = C_m \frac{dV_m}{dt} + g_K n^4\left(V_m - E_K\right) + g_{Na} m^3 h\left(V_m - E_{Na}\right) + G_L\left(V_m - E_L\right) \quad (8),$$

which can be rewritten in the following ordinary differential equation for

$$C_m \frac{dV_m}{dt} = g_{Na} m^3 h\left(E_{Na} - V_m\right) + g_K n^4\left(E_K - V_m\right) + G_L\left(E_L - V_m\right) + I_m . \quad (9)$$

If $p=(m, n, h)$ denotes the proportion of open gates of each type, the rate of gate opening and closing should respectively be α_p and β_p, which depend on the membrane potential V_m as follows

$$\underset{1-p}{\text{closed gates}} \underset{\beta_p}{\overset{\alpha_p}{\rightleftarrows}} \underset{p}{\text{open gates}} \quad (10),$$

with the rate variables α_p and β_p for each p given by

$$\left(\alpha_p, \beta_p\right) = \frac{A + Bv}{C + \exp\left(\frac{v + D}{F}\right)} \quad (11),$$

where $v = V_m - V_{rest}$ and A, B, C, D, and F are the coefficients listed in Table 1.

Table 1: The coefficients of α_p and β_p variables, chosen by the fitting of experimental data [3].

	A	*B*	*C*	*D*	*F*
α_m	2.5	-0.1	-1	-25	-10
α_n	0.1	-0.01	-1	-10	-10
α_h	0.07	0	0	0	20
β_m	4	0	0	0	18
β_n	0.125	0	0	0	80
β_h	1	0	1	-30	-10

The time derivative of the variable p is given by

$$\frac{dp}{dt} = \alpha_p\left(V_m\right)\left(1 - p\right) - \beta_p\left(V_m\right) p \quad .(12)$$

On defining the time scale and the steady state (asymptotic) value of the variable p by the relation

$$\tau_p\left(V_m\right) = \frac{1}{\alpha_p\left(V_m\right) + \beta_p\left(V_m\right)} \quad (13),$$

$$p_\infty\left(V_m\right) = \frac{\alpha_p\left(V_m\right)}{\alpha_p\left(V_m\right) + \beta_p\left(V_m\right)} \quad (14),$$

Eq. (12) is simplified to

$$\frac{dp}{dt} = \frac{p_\infty\left(V_m\right) - p}{\tau_p\left(V_m\right)} \quad (15),$$

with solution

$$p(t) = p_\infty\left(V_m\right) - \left[\, p_\infty\left(V_m\right) - p_0 \,\right] e^{-t/\tau_p\left(V_m\right)} \quad (16),$$

where p_0 is the resting constant of p.

In summary, according to this model, changes in the variables m, h and n are described in relation to the membrane potential V_m and time t after an electric stimulus has emerged. Eq. (15) for $p=(m,n,h)$ and the change of membrane potential V_m in relation to time t given by Eq. (9), comprise a non-linear dynamical system of 4 dimensions [2-9].

2.2. The Fitzhugh-Nagumo Model.

The H-H model describes quite accurately the action potential. It originates from the fitting of experimental data and reflects notions of cellular physiology, like ion channel structure and function. However, the study of its behavior in the four dimensions of the time dependent variables (V_m, m, h, n) is quite complicated. Therefore, various reduced models with similar behavior but fewer dimensions have been developed to facilitate the study of neuronal dynamics.

A characteristic of the H-H model is that the m variable changes much faster than the h and n variables (which have similar time constants) and the passive membrane voltage, when voltage-gated channels are closed. Thus,

$$0 < \tau_m\left(V_m\right) \ll \tau_v < \tau_n\left(V_m\right) \simeq \tau_h\left(V_m\right) \quad (17),$$

where $\tau_m(V_m)$, $\tau_n(V_m)$, and $\tau_h(V_m)$ the time constants for the m, n and h variables respectively, while the time constant for the passive membrane is

$$\tau_v = C_m G_L^{-1} \quad (18).$$

In consequence, m can be treated as an instantaneous variable approximated by its asymptotic value $m(t) \simeq m_\infty(V_m(t))$, under quasi-steady state approximation conditions. Furthermore, $n_\infty(V_m)$ and $1 - h_\infty(V_m)$ change in a similar way. Therefore, the h and n variables can be both linearly approximated by a single variable w [10]

$$w = k_1 - h \simeq k_2 n \quad (19),$$

where k_1, $k_2 > 0$ are constants. Then, the model can be adequately approximated by the following two ordinary differential equations

$$C_m \frac{dV_m}{dt} = g_{Na} m_\infty^3 (k_1 - w)(E_{Na} - V_m) + g_K (w/k_2)^4 (E_K - V_m) + G_L (E_L - V_m) + I_m \quad (20),$$

$$\frac{dw}{dt} = \frac{w_\infty - w(t)}{\tau_w} \quad (21).$$

A straight-forward generalization of Eqs. (20) and (21) lead to the following (non-dimensional) form

$$\frac{dv}{dt} = \frac{1}{\tau_v}\left[F(v,w) + RI\right] \quad (22),$$

$$\frac{dw}{dt} = \frac{1}{\tau_w} G(v,w) \quad (23),$$

where v is the non-dimensional form of membrane potential V_m, w is the recovery variable that represents both k_1-h and $k_2 n$, and $\tau_w > 0$. The functions $F(v, w)$ and $G(v, w)$ are defined accordingly [2, 8, 11-14].

Fitzhugh [15] was among the first to study numerically the dynamics of the H-H model and noticed that the variables follow fast (V_m and m) or slow (h and n) kinetics. He suggested one of the first two-dimensional models approximating the behavior of the H-H model. His model was based on the van der Pol oscillator equation [16] modified with Lienard transformation (with the addition of new coefficients) to read

$$\frac{dv}{dt} = -v^3(t) + (a+1)v^2(t) - av(t) - w(t) + I = v(t)\left[a - v(t)\right]\left[v(t) - 1\right] - w(t) + I \quad (24),$$

$$\frac{dw}{dt} = \varepsilon\left[bv(t) - \gamma w(t)\right] \quad (25).$$

He himself initially called this form of the model the Bonhoeffer-van der Pol model [17]. Almost simultaneously, Nagumo et al. [18] suggested an equivalent circuit model now commonly known as the Fitzhugh-Nagumo (F-N) model. This model is of the above generalized form given by Eqs. (22) and (23), where

$$F(v,w) = \tau_v\left[v(t)\left[a - v(t)\right]\left[v(t) - 1\right] - w(t)\right] \quad (26),$$

$$G(v,w) = bv - \gamma w \quad (27),$$

$$\tau_w = 1/\varepsilon \quad (28).$$

The F-N model can be treated analytically. Although not based exclusively on neurophysiological data, it approximates quite well the H-H model and maintains many of its properties, like the existence of a stable equilibrium, the excitability, the absence of all-or-none spikes, and the absence of a clearly defined threshold [8, 14, 19]. Therefore, it can be considered as a suitable representative of the H-H model [9].

In view of the above reduction, we proceed with the phase plane analysis of the F-N model. The variable $v(t)$ corresponds to the membrane potential V_m of the H-H model. It is the excitation variable and it changes according to the non-linear differential Eq. (24). On the other hand, $w(t)$, the recovery variable, corresponds to variables h and n and it changes according to the linear differential Eq. (25). Both equations are non-dimensional with the parameters a, b, γ and ε being constants. The parameter a, with $0 < a < 1$, defines the quasi-threshold of the model; $(b, \gamma) > 0$; and $0 < \varepsilon \ll 1$ defines the difference between the time scales of the two variables. The quantity I corresponds to the current I_m applied to the membrane during the neurophysiological experiments. The model is thus described by a continuous two-dimensional dynamical system.

Such a system can be conveniently studied through the analysis of its phase plane, that is the geometrical depiction of specific orbits, like the equilibria, the separatrices, and the limit cycles, that determine the topology of all other orbits, in the v-w plane [1, 2, 20]. In particular, for the w nullcline, we have

$$dw/dt = 0 \Rightarrow w = b/\gamma v \quad (29),$$

which on the v-w plane corresponds to a straight line that passes through (0, 0). Similarly, for the v nullcline, we have

$$dv/dt = 0 \Rightarrow w = v(a - v)(v - 1) + I \quad (30),$$

which on the v-w plane corresponds to a cubic curve with three arms, a left descending, a middle ascending and a right descending one. The local extrema of the curve consist of a local minimum

$$v_{\min} = \frac{1}{3}\left(1 + a - \sqrt{1 - a + a^2}\right) \quad (31),$$

between the left and the middle arm and a local maximum

$$v_{\max} = \frac{1}{3}\left(1 + a + \sqrt{1 - a + a^2}\right) \quad (32),$$

between the middle and the right arm. Consideration of the initial condition that $I = 0$ simplifies Eq. (30) to

$$w = v(a - v)(v - 1) \quad (33),$$

and the v axis is intercepted at the points where $v = 0$, $v = a$ and $v = 1$, corresponding to the left, middle and right arm respectively (Figure 1A).

In the general case, the two curves intercept each other at the points that satisfy the condition

$$b/\gamma v = v(a - v)(v - 1) \quad (34);$$

thus,

$$v(v - v_{i1})(v - v_{i2}) = 0 \quad (35),$$

where

$$v_{i1,i2} = \frac{1}{2}\left[1 + a \pm \sqrt{(1-a)^2 - 4b/\gamma}\right] \quad (36).$$

In consequence, if

$$(1-a)^2 > 4b/\gamma \quad (37),$$

the system would have three equilibria, (0, 0), (v_{i1}, b/γ v_{i1}) and (v_{i2}, b/γ v_{i2}). However, in the classical F-N model the parameters b and γ are chosen in a way that there is only the (0, 0) equilibrium, that is

$$(1-a)^2 < 4b/\gamma \quad (38),$$

and the system is monostable, as the neuron physiology suggests. At equilibrium, the Jacobian matrix of the linearized system is

$$\mathbf{L} = \begin{bmatrix} \frac{\partial(-av - w + I)}{\partial v} & \frac{\partial(-av - w + I)}{\partial w} \\ \frac{\partial\left[\varepsilon(bv - \gamma w)\right]}{\partial v} & \frac{\partial\left[\varepsilon(bv - \gamma w)\right]}{\partial w} \end{bmatrix} = \begin{bmatrix} -a & -1 \\ \varepsilon b & -\varepsilon\gamma \end{bmatrix} \quad (39),$$

with

$$tr\mathbf{L} = -a - \varepsilon\gamma < 0 \quad (40),$$

$$\det \mathbf{L} = a\varepsilon\gamma + \varepsilon b > 0 \quad (41).$$

Therefore, the equilibrium is asymptotically stable and its attraction domain extends to the whole plane. By further noting that

$$(tr\mathbf{L})^2 - 4\det\mathbf{L} = a^2 + 2a\varepsilon\gamma + \varepsilon^2\gamma^2 - 4a\varepsilon\gamma - 4\varepsilon b = (a-\varepsilon\gamma)^2 - 4\varepsilon b\,,$$ (42)

we can conclude that the equilibrium should be a "node" if

$$(a-\varepsilon\gamma)^2 - 4\varepsilon b > 0$$ (43),

and a "focus" if

$$(a-\varepsilon\gamma)^2 - 4\varepsilon b < 0$$ (44).

On the phase plane, $dw/dt < 0$ on the left and $dw/dt > 0$ on the right of the w nullcline. Respectively, $dv/dt < 0$ above (on the left of the middle arm) and $dv/dt > 0$ below the v nullcline (on the right of the middle arm).

The model is usually studied by considering $w(0) = 0$, while the stimulus is $v(0) = v_0$. If $v_0 < a$ (Figure 1A and 1B, point 1), then $dv/dt < 0$ and the orbit of the system returns to equilibrium (Figure 1A and 1B, the orbit in red). If $v_0 > a$ (Figure 1A and 1B, point 2), then $dv/dt > 0$ and v increases. The orbit of the system ends at the sole attractor without crossing the middle arm, which therefore has the character of a quasi-threshold. Instead, it travels for a longer distance on the plane, which is perceived as an excitation, before ending up at the equilibrium. Since $\varepsilon \ll 1$, the time scales between the two equations are separated, that is $dv/dt \gg dw/dt$. Therefore, at all points except the v nullcline, dw/dt is negligible in relation to dv/dt. In consequence, changes of w are slower than changes of v and the system is able to generate relaxation oscillations. The v nullcline is the unique set of points in which dw/dt is not negligible, because $dv/dt = 0$.

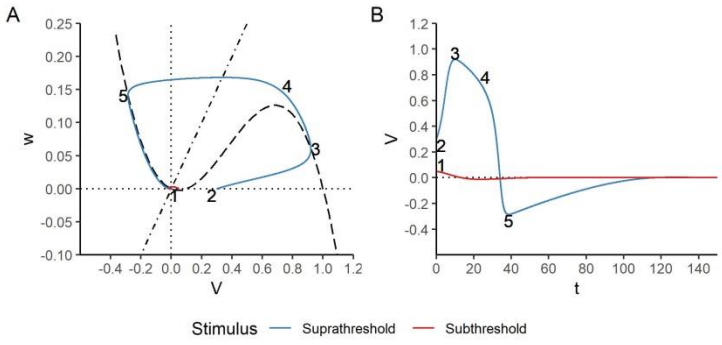

Figure 1. (A) Phase plane analysis for the F-N model. In dotted-dashed line is the w nullcline and in dashed line is the v nullcline. In red is an orbit starting under the threshold. In blue is an orbit starting over the threshold. (B) The evolution of v in time. The colors and the numbers correspond to those of (A).

The various stages of an excitation stem from the traits of the model, revealed by the phase plane analysis, as follows:

- Initially, for $a < v_0 < 1$, $dv/dt \gg 0$ and $dw/dt \cong 0$. The orbit reaches rapidly the right arm (Figure 1A and 1B, point 3), without significant deviations from the v axis.
- At the right arm the relations $dv/dt = 0$ and $dw/dt > 0$ hold. The orbit moves relatively slowly and close to the right arm until the local maximum (Figure 1A and 1B, point 4).
- At the local maximum the relations $dv/dt \ll 0$ and $dw/dt \cong 0$ hold. The orbit moves rapidly towards the left and in parallel to the v axis, as v increases and w remains almost stable.
- At last, at the left arm (Figure 1A and 1B, point 5), the relations $dv/dt = 0$ and $dw/dt < 0$ hold. The state returns slowly to the equilibrium [2, 8].

2.3. Propagation of Nerve Stimulation.

The action potential does not remain stationary after its generation. The polarity in neighbouring areas of the membrane is reversed due to the electric perturbation. As a result, the Na^+ voltage-sensitive channels in these areas open and the action potential gradually propagates along the axon. Meanwhile, the resting potential is restored at areas the stimulation has already passed through. The H-H and F-N models describe the potential and the currents locally at a single point of the membrane of the axon. The cable theory of Lord Kelvin, modified for the appendages of neurons, is used to study the propagation of the potential along the axon [21].

The system, regarding a cylindrical axon with cross section area A and diameter d, is characterized by:

- the cytoplasmic longitudinal resistance per unit of length of the axon

$$r = \frac{dR}{dx} = \frac{\tilde{r}}{A} = \frac{4\tilde{r}}{\pi d^2}$$ (45),

where $\tilde{r}$ is the special resistivity of the cytoplasm per unit of volume;

- the resistance of the membrane per unit of length

$$r_m = \frac{\tilde{r}_m}{\pi d}$$ (46),

where $\tilde{r}_m$ is the special resistivity of the membrane per unit of surface;

- the capacitance of the membrane per unit of length

$$c_m = \frac{dC_m}{dx} = \pi d\tilde{c}_m$$ (47),

where $\tilde{c}_m$ is the special capacitance per unit of surface of the membrane;

- the ion current that passes through the thickness of the membrane per unit of length, considered as a function of the membrane potential and time

$$j_{ion} = \frac{dI_m}{dx} = -\frac{f(V_m,t)}{r_m}$$ (48);

- the longitudinal (in the x direction) current i along the axon; and
- the propagation velocity c of the electric perturbation.

The cable equation, a special case of the reaction-diffusion equation, is expressed as

$$c_m\frac{\partial V}{\partial t} = \frac{1}{r}\frac{\partial^2 V}{\partial x^2} - j_{ion}$$ (49).

The time and space constants of the system are defined respectively by

$$\tau_c = r_m c_m$$ (50),

$$\lambda_c = \sqrt{\frac{r_m}{r}}$$ (51).

Another expression for the cable equation can be derived from Eq. (49) using Eqs. (50) and (51). It reads

$$\tau_c \frac{\partial V_m}{\partial t} = \lambda_c^2 \frac{\partial^2 V_m}{\partial x^2} - r_m j_{ion} \quad (52),$$

or, by using Eq. (48)

$$\tau_c \frac{\partial V_m}{\partial t} = \lambda_c^2 \frac{\partial^2 V_m}{\partial x^2} + f(V_m, t) \quad (53).$$

With regard to an active electric flow, as it applies to the axon according to the H-H model, the nonlinear differential equation

$$\tau_c \frac{\partial V_m}{\partial t} = \lambda_c^2 \frac{\partial^2 V_m}{\partial x^2} + f\left(V_m, m, n, h\right) \quad (54),$$

along with Eq. (12) hold. In the case of the F-N model, the electric flow is described by the equation

$$\tau_c \frac{\partial v}{\partial t} = \lambda_c^2 \frac{\partial^2 v}{\partial x^2} + f\left(v, w\right) \quad (55)$$

together with Eq. (12). For a traveling wave type solution, the propagation velocity c is constant and its non-dimensional form

$$C = \frac{c\tau_c}{\lambda_c} \quad (56)$$

is independent of time and position. Therefore, C depends only on the f function and the following equation

$$c = C\frac{\lambda_c}{\tau_c} = \frac{C}{c_m\sqrt{r_m r}} = \frac{C}{\pi d\tilde{c}_m\sqrt{\frac{\tilde{r}_m}{\pi d}\frac{4\tilde{r}}{\pi d^2}}} = \frac{C}{2\tilde{c}_m}\sqrt{\frac{d}{\tilde{r}_m\tilde{r}}} \quad (57),$$

holds. In other words, the propagation velocity is dependent on the properties of the cytoplasm, the membrane and the function that determines the membrane potential, as well as on the diameter of the axon [8, 22-26].

2.4. Coupled Electro-Mechanical Models.

The study of the influence of the mechanical deformation on the electrical behavior of the axon has led to (i) the development of models on the subcellular nanoscale level, in which the deformation of the membrane and the channels is observed; and (ii) the development of models at the micro/macroscale, in which the deformation of peripheral nerves and the central nervous system is observed. However, modeling of this coupling on the level of the neurophysiology and the function of the neuron is necessary, in order to bridge the gap between the nanoscale and the micro/macroscale. This task is undertaken here by focusing on specific generalizations of the F-N model. Analytical techniques, when feasible, are used for the study of the effects of the mechanical deformation on the behavior of the model. Numerical analysis was further performed with the XPPAUT 8.0 software (Ermentrout GB, 1996-2016) and the R 3.5.2 environment (R Core Team, 2018) with the deSolve 1.22 package (Sotaert K et al., 2010). The chosen values for the model parameters $a = 0.1$, $I = 0$, $\varepsilon = 0.01$, $b = 1$ and $\gamma = 2$ fulfill the conditions of the classical F-N model and have been used elsewhere in the literature as well [2].

2.4.1. Potential caused by deformation. The cellular membrane has the structure of a liquid crystal bilayer consisting of electrical dipoles, the lipids. By applying flexural deformation on the membrane, the orientation of the dipoles changes and electrical polarization between the surfaces of the membrane is created. As a result, a potential $V_f = f/\varepsilon_0\ 2H$ is observed, where f is a constant (flexocoefficient) depending on the composition of the membrane in lipids and proteins, ε_0 the dielectric constant in vacuum and H the mean curvature of the membrane [27]. In order to understand how this effect (i.e. flexoelectricity) can influence the generation and propagation of the action potential, we assume that V_f causes an equivalent current i_f and the F-N equations are modified to read $dv/dt = v(a - v)(v - 1) - w + I + i_f$ and $dw/dt = \varepsilon(bv - \gamma w)$. The new quantity i_f can be studied as an independent parameter with a linear dependence on dv/dt. Related analyses have been done in [28] by considering I as a bifurcation parameter.

The v nullcline follows the equation $w = v(a - v)(v - 1) + I + i_f$, while the w nullcline obeys the equation $w = b/\gamma\ v$. Consequently, the phase plane is similar to the phase plane of the F-N model, with the difference that the v nullcline is transposed higher by i_f. The two lines intercept only at the equilibrium. As i_f increases, for some value i_{f1}, the equilibrium becomes unstable and a limit cycle appears. For this value of i_f there is a Hopf bifurcation and the usual conditions

$$tr\mathbf{L} = 0 \quad (58),$$

$$\det\mathbf{L} > 0 \quad (59)$$

hold for the Jacobian matrix of the linearized system at equilibrium

$$\mathbf{L} = \begin{bmatrix} -3v^2 + 2(1+a)v - a & -1 \\ \varepsilon b & -\varepsilon\gamma \end{bmatrix} \quad (60).$$

Therefore,

$$tr\mathbf{L} = 3v^2 - 2(1+a)v + a + \varepsilon\gamma = 0 \quad (61),$$

with solutions

$$v_{h1,}v_{h2} = \frac{1}{3}(1 + a \pm \sqrt{1 - a + a^2 - 3\varepsilon\gamma}) \quad (62).$$

It follows that, for the values

$$i_{f1,f2} = -v_{h1,h2}(a - v_{h1,h2})(v_{h1,h2} - 1) + \frac{b}{\gamma}v_{h1,h2} \quad (63),$$

a Hopf bifurcation appears at the point $(v, w) = (v_{h1,h2}, b/\gamma\ v_{h1,h2})$, while between the two values the equilibrium is unstable. At the first bifurcation point the inequality

$$v_{h1} = \frac{1}{3}(1 + a - \sqrt{1 - a + a^2 - 3\varepsilon\gamma}) > \frac{1}{3}(1 + a - \sqrt{1 - a + a^2}) = v_{\min} \quad (64),$$

holds and the equilibrium lies on the middle arm and slightly on the right of the local minimum. Similarly, at the second bifurcation point the inequality

$$v_{h2} = \frac{1}{3}(1 + a - \sqrt{1 - a + a^2 - 3\varepsilon\gamma}) < \frac{1}{3}(1 + a - \sqrt{1 - a + a^2}) = v_{\max} \quad (65)$$

holds and the equilibrium lies on the middle arm and slightly on the left of the local maximum.

Numerical analysis of the model was carried out, by viewing i_f as the bifurcation parameter. The bifurcation diagram for the modified F-N model with i_f as the bifurcation parameter is depicted in Figure 2. Points 1 ($v = 0.05931$ and $i_f = 0.03193$) and 2 ($v = 0.674$ and $i_f = 0.2109$) denote a Hopf bifurcation and validate the analytically computed values. In the region of periodic solutions, two values of v correspond to every value of i_f: the maximum and the minimum values of v for each limit cycle. The phase plane at the two Hopf bifurcation points is depicted in Figure 3A and 3B. A periodic solution of the system in time for $V_{f1} < V_f < V_{f2}$ is depicted in Figure 3C.

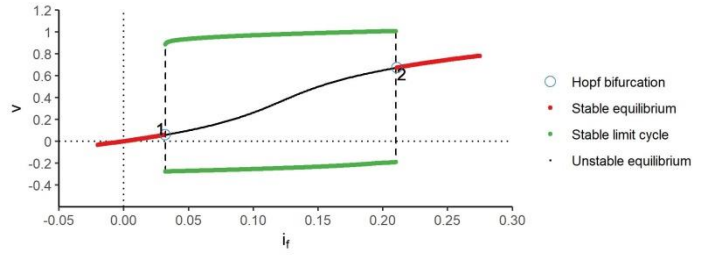

Figure 2. Bifurcation diagram for the modified F-N model with i_f as the bifurcation parameter. The equilibria (red line for asymptotically stable; black line for unstable equilibria), the stable limit cycles (green lines) generating periodic solutions, and the Hopf bifurcations (blue circles) are shown.

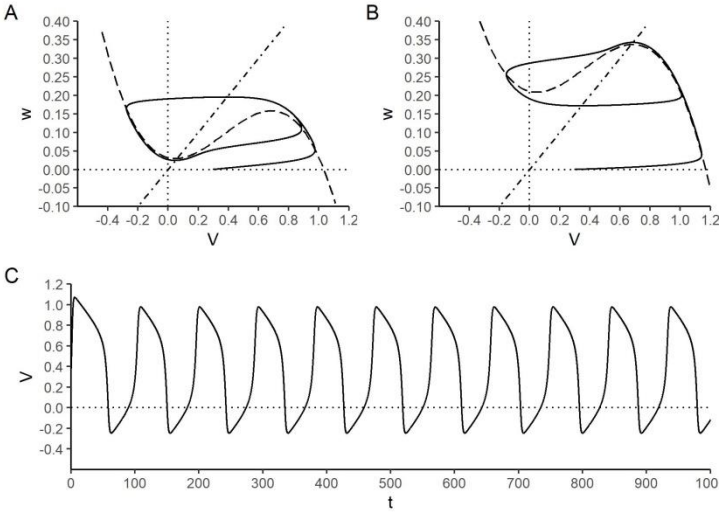

Figure 3. (A) Phase plane at the Hopf bifurcation point for $i_f = i_{f1}$. (B) Phase plane at the Hopf bifurcation point for $i_f = i_{f2}$. (C) The evolution of v in time: periodic solutions of the modified F-N system.

2.4.2. Deformation Effects on the Kinetics of K^+ Channels.

(i) K^+ channels activated and inactived by tensile deformation: The discovery of the mechanosensitivity of the ion channels led to the study of the influence of the mechanical deformation of the membrane on the kinetics of the electrosensitive K^+ channels. In some types of these channels the application of tensile deformation (stretch) in the initial stages of their activation, when they are closed, accelerates their activation. Conversely, when tensile deformation is applied in the final stages of their activation, it accelerates their inactivation [29]. Furthermore, these effects have a dose-depended behavior. Therefore, the changes in the activity of the channels are greater and faster with increased membrane deformation, until the membrane ruptures.

The effect of tensile deformation could be represented in the setting of the F-N model with an increase in the slow subsystem time scale ε. Consequently, the separation of time scales between the fast and the slow subsystem would be attenuated and the ability for the generation of relaxation oscillations would be lost. More specifically, as dw/dt would now be comparable with dv/dt, an excitation with $v_0 > a$ would not proceed in parallel with the v axis and it would cross the middle arm to reach equilibrium. The result, in consequence, would be a minimization of the maximal stimulation of v and a faster restoration to equilibrium. Numerical simulations for various values of ε were carried out, which confirmed the gradual loss of excitability and blurring of the threshold as ε increases (Figure 4A and 4B). Furthermore, in addition to the decrease of the height of the pulse when ε is increased, the decrease of the restoration time to equilibrium was also noticed, as the relaxation variable w followed a time scale evolution similar to v. These effects were not due to the appearance of a bifurcation, but to the loss of time scale separation.

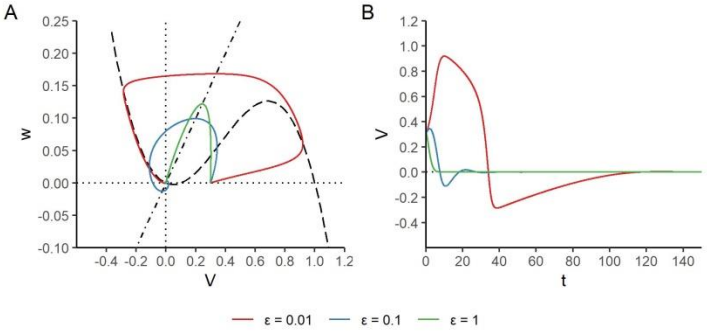

Figure 4. (A) Phase plane of the modified F-N model with orbits emerging from a point over the threshold for various values of ε. (B) The time evolution of v for a stimulus $v_0 > \alpha$ for various values of ε.

(ii) Appearance of time delay in the Fitzhugh-Nagumo model: Although the mechanical deformation causes acceleration of the activation and inactivation in some types of voltage-sensitive K^+ channels, in other types it causes delay of their activation [30]. In these channels, the voltage-sensitive domain (VSD) is distinct from the pore domain (PD). According to recent molecular dynamics models, the two domains are not in direct contact when the channels are closed. More specifically, during activation, the movement of the positively charged S4 helix, which belongs to the VSD, initially causes stretching of the S4-S5 linker, which connects the two domains. Eventually, the entire VSD moves, so that it gets in contact with the PD, resulting to further stretching of the S4-S5 linker and opening of the channel [31]. The tensile deformation of the membrane could cause delay in the movement of the VSD near the PD, as the VSD lies lateral to the PD and in close contact with the lipids of the membrane. Furthermore, it has been noticed that high hydrostatic pressure slows the kinetics of the ion channels, without influencing their conductance [32-34].

These effects could be modeled in the F-N equations as a time delay τ in the w variable. Then Eq. (24) could be modified to read

$$\frac{dv}{dt} = v(t)\left[a - v(t)\right]\left[v(t) - 1\right] - w(t-\tau) + I \qquad (66).$$

Analytical solutions of dynamical systems of time delay differential equations and respective bifurcation properties are rather complicated, although some aspects of their behavior have been studied case by case. Accordingly, modified F-N models have been studied numerically in order to explain the influence of alcohol on neurons [35]. Our own, numerical analyses were carried out for $v_0 = 0$, 0.05, and 0.3 and $\tau = 0$, 5, 10, 15, and 20. For $v_0 = 0$, no shift of the state of the system from the equilibrium was observed, as expected. For $v_0 = 0.05 < a$, stable limit cycles of small amplitude for $\tau = 15$ and large amplitude for $\tau = 20$ were observed, while for smaller time delays the system executed damped oscillations around the equilibrium (Figure 5A and 5B). For $v_0 = 0.3 > a$, stable limit cycles of large amplitude for $\tau = 15$ and 20 were generated. The amplitude of the oscillation gradually increased with an increase in τ. For smaller time delays the system exhibits damped oscillations around the equilibrium (Figure 5C and 5D).

2.4.2. Changes in the Conduction Velocity. Apart from local effects that may influence the generation and propagation of the action potential, the mechanical deformation of the axon could affect its propagation by altering the conduction velocity. According to the cable theory, in a cylindrical axon with length l and diameter d the conduction velocity is given by Eq. (57). The volume of axon

$$V = \frac{\pi}{4} d^2 l \quad (67),$$

is considered stable. Therefore, if tensile deformation (that is lengthening) is applied to the axon, its diameter

$$d = 2\sqrt{\frac{V}{\pi l}} \quad (68),$$

will be reduced, resulting in the reduction of the action potential conduction velocity

$$c = \frac{C}{\tilde{c}_m}\sqrt{\frac{1}{2\tilde{r}_m \tilde{r}}}\left(\frac{V}{\pi}\right)^4 l^{-4} \quad (69).$$

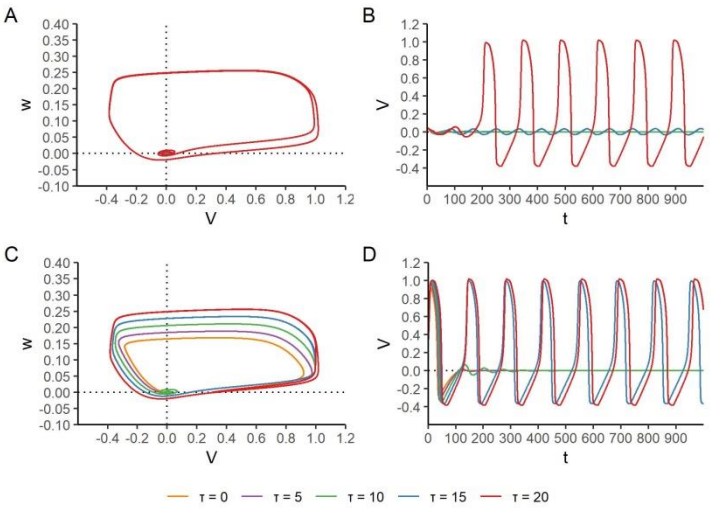

Figure 5. (A) Orbits in the modified F-N model for $v_0 = 0.05$. (B) The evolution of v in time in the modified FHN model for $v_0 = 0.05$. (C) Orbits in the modified F-N model for $v_0 = 0.3$. (D) The time evolution of v in the modified F-N model for $v_0 = 0.3$.

3. RESULTS SECTION

(i) Macroscopic experiments supporting Electro-Mechanical Models: Modeling the influence of mechanical deformation to the generation and propagation of the action potential is encouraged by the results of macroscopic experiments. Most of these have been conducted on peripheral nerves, as the study of the mechanical deformation and the electrical activity of the axons is easier. Nevertheless, the development of methods for the study of such effects in the central nervous system, although more difficult, is imperative, in order to investigate the impact of non-destructive mechanical deformation on the function of neurons under conditions of increased intracranial pressure.

In this connection, it is pointed out that Wall et al. [36] noticed a reversible reduction in the compound action potential (CAP) amplitude for a 6 % elongation of rabbit tibial nerves in stretching experiments *in vivo*, which is under the ischemia limit and without structural changes of the nerves. Similarly, Ochs et al. [37] performed *in vitro* stretching experiments on canine peroneal nerves and rat sciatic nerves. After the possibility of nerve ischemia and hypoxia was excluded, a reversible (for a small deformation) reduction in the CAP amplitude and beading appearance of axons were observed. As a result, according to those researchers, the longitudinal resistance of axons was increased. To the contrary, an increase of the amplitude was observed in some experiments. In another study, Li and Shi [38] observed a reversible 16 % reduction of the CAP amplitude for deformation of 5 % in *ex vivo* stretching experiments on guinea-pig tibial and peroneal nerves, as well as a reduction of the conduction velocity, proportional to the deformation. Furthermore, they noticed that, during prolonged deformation, part of the nerve function was restored, which indicates the existence of mechanisms for the relaxation of mechanical stress. It should be noted that the possibility of ischemia was excluded in these experiments as well, while the local deformation was also studied and found inhomogeneous. Finally, Stecker et al. [39] observed an increase in the conduction velocity for small deformations in some cases of similar experiments, which was attributed to increased axon excitability.

(ii) Clinical importance of electro-mechanical models: According to our and previous analytical / numerical studies regarding the influence of mechanical deformation on the generation and propagation of the action potential, it becomes evident that coupled electro-mechanical models can constitute a substrate for further study of the relationship between mechanical and electrical properties of neurons. Moreover, the necessity for the development of such models becomes clear in view of results of experiments that isolate the non-destructive mechanical deformation of the axon from other factors that may influence its function, like ischemia. According to the models studied in the present work, the influence of the mechanical deformation, due to the effects of flexoelectricity, the deformation of potassium channels or the change of axon dimensions, may either have inhibitory activity on the generation and propagation of the action potential, or cause the tonic stimulation of the neuron. Clinically, both effects would prevent the successful transmission of information that characterizes the neuron, which means that they would be expressed pathologically, depending on the number of cells that would participate.

(iii) Possible extensions of the present work: It is obvious that a meticulous study for each of the new effects considered heirein at all scales of observation is necessary. For example, at the nanoscale, the clarification of the structure of the Na^+ and K^+ channels is necessary both in the open and the closed conformation. Moreover, the study of the mechanical properties of channels, the membrane, the cytoskeleton and more complex structures is necessary, perhaps utilizing methods like atomic force microscopy (AFM). The analysis of the transition between open and closed conformations, as well as the influence of mechanical stress on channels and the membrane can be achieved with molecular dynamics, while the contribution of the cytoskeleton should also be taken into account. It should be noted that models for the contribution of the membrane deformation on the function

of the channels have already been proposed [40-42] and they could be extended to take into account the evolution of the action potential in time. The contribution of the flexoelectricity may be studied with techniques like patch clamping and AFM. The coupling of mechanical and electrical properties can initially be achieved with modifications in the parameters of simpler models, like the F-N model, which was used in the present work. Subsequently, it can be studied for more complex models, like the H-H model, for example with alterations in parameters concerning the Na^+ and K^+ channels. The combination of such models with cable theory would also be interesting, in order to study the impact of mechanical deformation on the propagation of the action potential. Moreover, the consideration of models that propose the companion of the propagated action potential by a mechanical wave [43] could provide further insight into the interaction between the electrical and the mechanical behavior of the axon. It should be underlined that, in the present work, only the mechanical deformation and the electric properties of the unmyelinated axon were taken into account. However, their study in myelinated nerve fibers, as well as in other elements of the neuron, would also be useful, in order to analyze the impact of the mechanical deformation on arrays of cells and neural circuits. Furthermore, the presence of glia and the influence of mechanical deformation on its glial and neuronal function should be taken into account. Finally, the study of such effects at the macroscopic scale would also be important, by considering the change of the macroscopic conductance for various types of mechanical deformation.

4. CONCLUSIONS

The generation and propagation of the action potential along the axon are described adequately by neurophysiological models like the H-H and F-N models and the cable theory. Such models are used by neuroscientists to approach the function of the neuron and, by extension, neural circuits and the nervous system as a whole. The mechanical properties of the nervous tissue have also been studied, to a degree, mainly in the context of traumatic injury. However, the influence of the mechanical deformation on the electric behavior of the nervous system has not been studied thoroughly, with the exception of experiments on subcellular structures and some macroscopic experiments on peripheral nerves. Herein, we presented electromechanical models for the nerve stimulation propagation by taking into account the effects of flexoelectricity, as well as axon, cellular membrane and potassium channels deformation. It becomes evident that the study of the interaction of the electric and the mechanical properties of the neural tissue is a field with notably useful clinical applications, particular difficulties in its study, but also wide perspectives for further research.

5. REFERENCES

[1] S. L. Campbell, R. Haberman, *Introduction to Differential Equations: with Dynamical Systems*. Princeton University Press, **2008.**

[2] E. M. Izhikevich, *Dynamical Systems in Neuroscience. The Geometry of Excitability and Bursting*. The MIT Press, **2007.**

[3] A. L. Hodgkin, A. F. Huxley, A quantitative description of membrane current and its application to conduction and excitation in nerve. *J. Physiol.*, 117, 4, 500-544, **1952**, https://doi.org/10.1113/jphysiol.1952.sp004764.

[4] A. L. Hodgkin, A. F. Huxley, Currents carried by sodium and potassium ions through the membrane of the giant axon of Loligo. *J. Physiol.*, 116, 4, 449-472, **1952**, https://doi.org/10.1113/jphysiol.1952.sp004717.

[5] A. L. Hodgkin, A. F. Huxley, The components of membrane conductance in the giant axon of Loligo. *J. Physiol.*, 116, 4, 473-496, **1952**, https://doi.org/10.1113/jphysiol.1952.sp004718.

[6] A. L. Hodgkin, A. F. Huxley, The dual effect of membrane potential on sodium conductance in the giant axon of Loligo. *J. Physiol.*, 116, 4, 497-506, **1952**, https://doi.org/10.1113/jphysiol.1952.sp004719.

[7] A. L. Hodgkin, A. F. Huxley, Propagation of electrical signals along giant nerve fibres. *Proc. R. Soc. Lond. B. Biol. Sci.*, 140, 177-183, **1952**, https://doi.org/10.1098/rspb.1952.0054.

[8] J. Keener, J. Sneyd, *Mathematical Physiology*, *2nd ed*. Springer Science+Business Media, LLC, **2009**, https://doi.org/10.1007/978-0-387-75847-3.

[9] J. D. Murray, *Mathematical Biology. I. An Introduction, 3rd ed*. Springer Science+Business Media, LLC, **2002**, https://doi.org/10.1007/b98868.

[10] V. I. Krinskii, Y. M. Kokoz, Analysis of equations of excitable membranes - I. Reduction of the Hodgkin-Huxley equations to a second order system. *Biofizika*, 18, 506-511, **1973**

[11] W. Gerstner, W. Kistler, *Spiking Neuron Models: Single Neurons, Populations, Plasticity*. Cambridge University Press, **2002.**

[12] L. F. Abbott, T. Kepler, B. Model Neurons: From Hodgkin-Huxley to Hopfield. In *Statistical Mechanics of Neural Networks: Proceedings of the XIth Sitges Conference, Sitges, Barcelona, Spain, 3-7 June 1990*. Garrido L, Ed. Springer, pp. 5-18, **1990**, https://doi.org/10.1007/3-540-53267-6.

[13] B. Alberts, A. Johnson, J. Lewis, M. Raff, K. Roberts, P. Walter, *Molecular Biology of the Cell, 5th ed*. Garland Science, **2008.**

[14] W. Gerstner, W. M. Kistler, R. Naud, L. Paninski, *Neuronal Dynamics. From Single Neurons to Networks and Models of Cognition*. Cambridge University Press, **2014.**

[15] R. Fitzhugh, Mathematical models of threshold phenomena in the nerve membrane. *Bull. Math. Biophys.*, 17, 257-278, **1955**, https://doi.org/10.1007/BF02477753.

[16] B. van der Pol, A theory of the amplitude of free and forced triode vibrations. *Radio Review*, 1, 701-710, 754-762, **1920.**

[17] R. Fitzhugh, Impulses and physiological states in theoretical models of nerve membrane. *Biophys. J.*, 1, 445-466, **1961**, https://doi.org/10.1016/s0006-3495(61)86902-6.

[18] J. Nagumo, S. Arimoto, S. Yoshizawa, An active pulse transmission line simulating nerve axon. *Proc. IRE*, 50, 10, 2061-2070, **1962**, https://doi.org/10.1109/JRPROC.1962.288235.

[19] J. Rinzel, Electrical excitability of cells, theory and experiment: review of the Hodgkin-Huxley foundation and an update. *Bull. Math. Biol.*, 52, 1/2, 5-23, **1990**, https://doi.org/10.1016/S0092-8240(05)80003-5.

[20] S. H. Strogatz, *Nonlinear Dynamics and Chaos. With Applications to Physics, Biology, Chemistry, and Engineering*. Perseus Books Publishing, **1994.**

[21] W. Thomson, On the theory of the electric telegraph. *Proc. R. Soc.*, 7, 382, **1855.**
[22] A. Scott, *Neuroscience: A Mathematical Primer*. Springer-Verlag, **2002**, https://doi.org/10.1007/b98897.
[23] K. S. Cole, A. L. Hodgkin, Membrane and protoplasm resistance in the squid giant axon. *J. Gen. Physiol.*, 22, 671-687, **1939**, https://doi.org/10.1085/jgp.22.5.671.
[24] W. Rall, Branching dendritic trees and motoneuron membrane resistivity. *Exp. Neurol.*, 1, 5, 491-527, **1959**, https://doi.org/10.1016/0014-4886(59)90046-9.
[25] A. L. Hodgkin, W. A. Rushton, The electrical constants of a crustacean nerve fibre. *Proc. R. Soc. Lond. B. Biol. Sci.*, 133, 873, 444-479, **1946**, https://doi.org/10.1098/rspb.1946.0024.
[26] J. D. Murray, *Mathematical Biology. II. Spatial Models and Biomedical Applications, 3rd ed.* Springer Science+Business Media, LLC, **2003**, https://doi.org/10.1007/b98869.
[27] A. G. Petrov, F. Sachs, Flexoelectricity and elasticity of asymmetric biomembranes. *Phys. Rev. E Stat. Nonlin. Soft Matter Phys.*, 65, 021905, **2002**, https://doi.org/10.1103/PhysRevE.65.021905.
[28] W. C. Troy, Bifurcation phenomena in Fitzhugh's nerve conduction equations. *J. Math. Anal. Appl.*, 54, 3, 678-690, **1976**, https://doi.org/10.1016/0022-247X(76)90187-6.
[29] C. X. Gu, P. F. Juranka, C. E. Morris, Stretch-activation and stretch-inactivation of Shaker-IR, a voltage-gated K^+ channel. *Biophys. J.*, 80, 2678-2693, **2001**, https://doi.org/10.1016/S0006-3495(01)76237-6.
[30] U. Laitko, P. F. Juranka, C. E. Morris, Membrane stretch slows the concerted step prior to opening in a Kv channel. *J. Gen. Physiol.*, 127, 6, 687-701, **2006**, https://doi.org/10.1085/jgp.200509394.
[31] M. O. Jensen, V. Jogini, D. W. Borhani, A. E. Leffler, R. O. Dror, D. E. Shaw, Mechanism of voltage gating in potassium channels. *Science*, 336, 229-233, **2012**, https://doi.org/10.1126/science.1216533.
[32] A. G. MacDonald, Ion channels under high pressure. *Comp. Biochem. Physiol. A Mol. Integr. Physiol.*, 131, 3, 587-593, **2002**, https://doi.org/10.1016/S1095-6433(01)00510-4.
[33] F. Conti, R. Fioravanti, J. R. Segal, W. Stuhmer, Pressure dependence of the potassium currents of squid giant axon. *J. Membr. Biol.*, 69, 35-40, **1982**, https://doi.org/10.1007/BF01871239.
[34] F. Conti, R. Fioravanti, J. R. Segal, W. Stuhmer, Pressure dependence of the sodium currents of squid giant axon. *J. Membr. Biol.*, 69, 23-34, **1982**, https://doi.org/10.1007/BF01871238.
[35] R. S. Franca, I. E. Prendergast, E.-S. Sanchez, M. Sanchez, F. Berezovsky,The Role of Time Delay in the Fitzhugh-Nagumo Equations: The Impact of Alcohol on Neuron Firing. Technical Report, Report No. BU-1577-M, **2001**
[36] E. J. Wall, J. Massie, B., M. K. Kwan, B. L. Rydevik, R. R. Myers, S. R. Garfin, Experimental stretch neuropathy. Changes in nerve conduction under tension. *J. Bone Joint Surg. Br.*, 74, 126-129, **1992**
[37] S. Ochs, R. Pourmand, K. Si, R. N. Friedman, Stretch of mammalian nerve in vitro: effect on compound action potentials. *J. Peripher. Nerv. Syst.*, 5, 4, 227-235, **2000**, https://doi.org/10.1111/j.1529-8027.2000.00025.x.
[38] J. Li, R. Shi, Stretch-induced nerve conduction deficits in guinea pig ex vivo nerve. *J. Biomech.*, 40, 3, 569-578, **2007**, https://doi.org/10.1016/j.jbiomech.2006.02.009.
[39] M. M. Stecker, K. Baylor, J. Wolfe, M. Stevenson, Acute nerve stretch and the compound motor action potential. *J. Brachial Plex. Peripher. Nerve. Inj.*, 6, 1, 4, **2011**, https://doi.org/10.1186/1749-7221-6-4.
[40] D. Reeves, T. Ursell, P. Sens, J. Kondev, R. Phillips, Membrane mechanics as a probe of ion-channel gating mechanisms. *Phys. Rev. E*, 78, 041901, **2008**, https://doi.org/10.1103/PhysRevE.78.041901.
[41] R. Phillips, T. Ursell, P. Wiggins, P. Sens, Emerging roles for lipids in shaping membrane-protein function. *Nature*, 459, 7245, 379-385, **2009**, https://doi.org/10.1038/nature08147.
[42] T. Ursell, K. C. Huang, E. Peterson, R. Phillips, Cooperative gating and spatial organization of membrane proteins through elastic interactions. *PLoS Comput. Biol.*, 3, 5, e81, **2007**, https://doi.org/10.1371/journal.pcbi.0030081.
[43] A. El Hady, B. B. Machta, Mechanical surface waves accompany action potential propagation. *Nat. Commun.*, 6, 6697, **2015**, https://doi.org/10.1038/ncomms7697.

6. ACKNOWLEDGEMENTS

This work is, in part, a result of the first author's Master Thesis at the Lab of Mechanics and Materials (LMM).